RAA 2017 Vol. **17** No. **4**, 31 (6pp) doi: 10.1088/1674–4527/17/4/31

http://www.raa-journal.org *http://iopscience.iop.org/raa*

***R**esearch in*
***A**stronomy and*
***A**strophysics*

LETTERS

Can the temperature of Ellerman Bombs be more than 10 000 K?

Cheng Fang, Qi Hao, Ming-De Ding and Zhen Li

School of Astronomy and Space Science, Nanjing University, Nanjing 210093, China; *fangc@nju.edu.cn*
Key Laboratory of Modern Astronomy and Astrophysics (Nanjing University), Ministry of Education, Nanjing 210023, China
Collaborative Innovation Center of Modern Astronomy and Space Exploration, Nanjing 210023, China

Received 2017 January 3; accepted 2017 February 5

Abstract Ellerman bombs (EBs) are small brightening events in the solar lower atmosphere. By their original definition, the main characteristic of EBs is the two emission bumps in both wings of chromospheric lines, such as Hα and Ca II 8542 Å lines. Up to now, most authors have found that the temperature increase of EBs around the temperature minimum region is in the range of 600–3000 K. However, with recent IRIS observations, some authors proposed that the temperature increase of EBs could be more than 10 000 K. Using non-LTE semi-empirical modeling, we investigate the line profiles, continuum emission and radiative losses for EB models with different temperature increases, and compare them with observations. Our result indicates that if the EB maximum temperature reaches more than 10 000 K around the temperature minimum region, then the resulting Hα and Ca II 8542 Å line profiles and the continuum emission would be much stronger than those of EB observations. Moreover, due to the high radiative losses, a high temperature EB would have a very short lifetime, which is not compatible with observations. Thus, our study does not support the proposal that EB temperatures are higher than 10 000 K.

Key words: line profiles — Sun: photosphere — Sun: chromosphere

1 INTRODUCTION

Ellerman bombs (EBs: Ellerman 1917) are small-scale brightening events in the solar lower atmosphere. Their characteristic feature is the excess emission in the wings of chromospheric lines, such as Hα and Ca II 8542 Å lines. Using high spatial resolution data, it was found that the lifetime of EBs is 2–20 minutes, and their size can be smaller than 1″ (Vissers & Rouppe van der Voort 2012; Nelson et al. 2013; Li et al. 2015). The temperature increase of EBs around the temperature minimum region (TMR) is about 600–1500 K (Georgoulis et al. 2002; Fang et al. 2006; Hong et al. 2014; Berlicki & Heinzel 2014). Recently, using high-resolution Hα and Ca II 8542 Å spectra obtained by the 1.6 m New Solar Telescope (NST), Li et al. (2015) found that the temperature increase can be about 3000 K even for three of the smallest EBs. The energy of EBs is estimated to be in the range of 10^{25}–10^{27} erg (e.g. Georgoulis et al. 2002; Fang et al. 2006; Li et al. 2015). It should be emphasized that there are some "pseudo-EBs" which are bright points in some images, but probably manifestations of deep radiation escape (Rutten et al. 2013; Vissers et al. 2015). Thus, the best way to identify EBs is by using spectral data.

Recently, with the Interface Region Imaging Spectrograph (IRIS; De Pontieu et al. 2014), some authors found that there are small-scale bright regions observed in 1400 Å and 1330 Å images, called IRIS bombs (IBs) (Peter et al. 2014; Tian et al. 2016), which have local heating in the photosphere up to $\sim 8 \times 10^4$ K under the assumption of collisional ionization equilibrium (Peter et al. 2014) or $1-2\times10^4$ K under the local thermo-

dynamic equilibrium (LTE) assumption (Rutten 2016). Thus, the relationship between EBs and IBs becomes an interesting question. Vissers et al. (2015) studied five EBs and found that strong EBs can produce IB-type spectra. Kim et al. (2015) also found the connection between an IB and an EB. Recently, Tian et al. (2016) used IRIS and Chinese New Vacuum Solar Telescope (NVST; Liu et al. 2014) data, and identified 10 IBs. Among them, three are obvious and three others are possibly connected to EBs, but the remaining four IBs are not EBs. They concluded that some EBs connected to IBs can be heated to $1 \sim 8 \times 10^4$ K, which is much hotter than what can be obtained from non-LTE modeling of EBs. Thus, whether EBs can be heated to such a high temperature is a hot topic.

In this paper, we use non-LTE modeling to investigate some characteristics of EB models with different temperatures, and compare them with observations, which were performed with the largest aperture solar telescope in the world, the 1.6 m off-axis NST (Goode & Cao 2012; Cao et al. 2010) at Big Bear Solar Observatory (BBSO). The method of non-LTE modeling is described in Section 2. The resulting characteristics of EB models are given in Section 3. General discussion and conclusion are provided in Section 4.

2 SEMI-EMPIRICAL MODELING OF EBS WITH DIFFERENT TEMPERATURES

We use the non-LTE method as described in the paper Fang et al. (2006). That is, prescribing a semi-empirical temperature distribution for an EB model, we solve the statistical equilibrium equation, the radiative transfer equation, the hydrostatic equilibrium and the particle conservation equations iteratively. A four-level hydrogen atom and a five-level Ca II atom are taken. All the bound-free and free-free transitions of the hydrogen atom and negative hydrogen (H^-) are included. The convergence criterion is that the relative difference of the mean intensities between the last two iterations is less than 10^{-7} and 10^{-9} for hydrogen and calcium atoms, respectively. Then the Hα and Ca II 8542 Å line profiles and continuum intensity can be calculated.

As typical cases, we take three EB models with different temperatures around the TMR. The models labeled EB15000 and EB10000 have a maximum temperature of 15 000 K and 10 000 K, respectively. The third one labeled EB0955 has a maximum temperature of 7000 K, which is about the same as that given by the empirical model labeled No.2 EB in our recent paper of Li et al. (2015). The empirical model of EB0955 can reproduce well the Hα and Ca II 8542 Å line profiles observed by the Fast Imaging Solar Spectrograph (FISS) (Chae et al. 2013) of BBSO/NST on 2013 June 6 at 09:55 UT. Compared with the VALC quiet-Sun model (Vernazza et al. 1981), the temperature increases for the three EB models are 11 000 K, 6000 K and 3000 K, respectively.

Figure 1 gives the temperature distributions for the three models. For comparison, we also plot the temperature distributions in the semi-empirical model for plages (denoted by "Plage") given by Fang et al. (2001) and for the VALC quiet-Sun model (denoted by "VALC"). In the figure, M is the column mass density.

Figure 2 gives both the observed and computed Hα and Ca II 8542 Å line profiles for the three EB models. It can be seen that the computed profiles of the EB0955 can match the observed ones well, but those of the EB10000 and EB15000 are much stronger and broader than what is given by observations.

Using the non-LTE method mentioned above, we can calculate the continuum emission for the three models. Figure 3 gives the result. It can be seen that the continuum emissions of EB10000 and EB15000 are much stronger than that of EB0955. Particularly, there would be a very strong Balmer jump for both EB10000 and EB15000. Obviously, such strong continuum emissions and very strong Balmer jump are never observed in the spectra of EBs.

3 RADIATIVE LOSSES

We can further estimate the radiative losses of the three EB models by using non-LTE modeling. The method is similar to that in Fang et al. (2006). That is, considering that the main heating regions of three EB models are around the TMR, we can use the following equation to estimate the total radiative losses $E_{\rm r}$ of the EB models

$$E_{\rm r} = DA_{\rm EB}\frac{R_{\rm EB}}{4}\ , \tag{1}$$

where

$$R_{\rm EB} = \int_{h_1}^{h_2} R_{\rm r}\, dh$$

is the height-integrated radiative cooling rate per unit area in the main heating region [h_1, h_2]. h_1 and h_2 are the lower and upper heights of the heated region, respectively. $R_{\rm r}$ is the peak rate of radiative losses in units of erg cm^{-3} s^{-1}. Considering that the rate of radiative

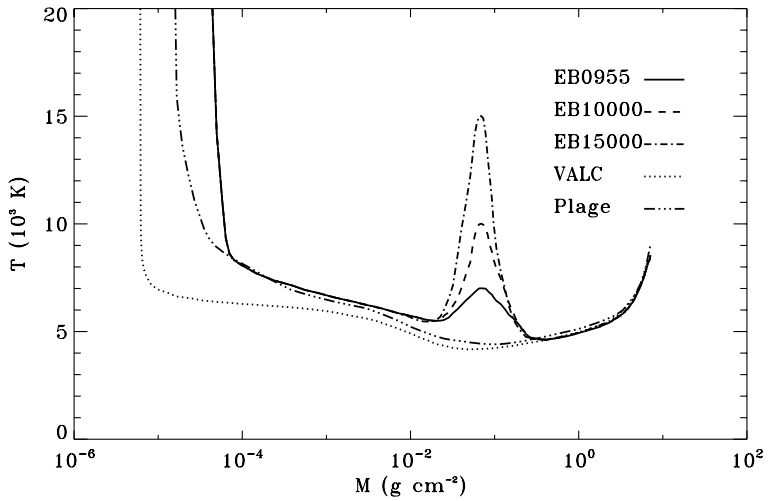

Fig. 1 Temperature distributions in the three EB models: EB0955 (*solid line*), EB10000 (*dashed line*) and EB15000 (*dash-dotted line*), compared to that of the plage model (*dash three-dotted line*) given by Fang et al. (2001), and that of the quiet-Sun model (i.e., the VALC model, *dotted line*) given by Vernazza et al. (1981).

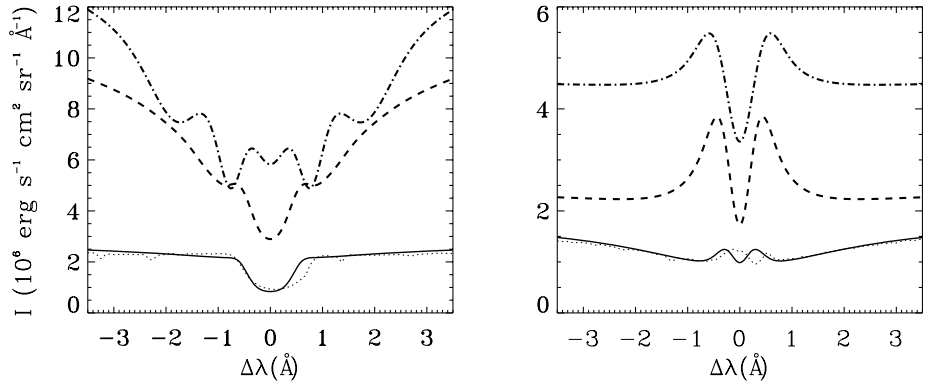

Fig. 2 Comparison between the observed (*dotted lines*) and computed Hα (*left*) and Ca II 8542 Å (*right*) line profiles for the EB0955 (*solid lines*), the EB10000 (*dashed lines*) and the EB15000 (*dash-dotted lines*). All theoretical profiles are convolved with a macroturbulence velocity of 8 km s^{-1}.

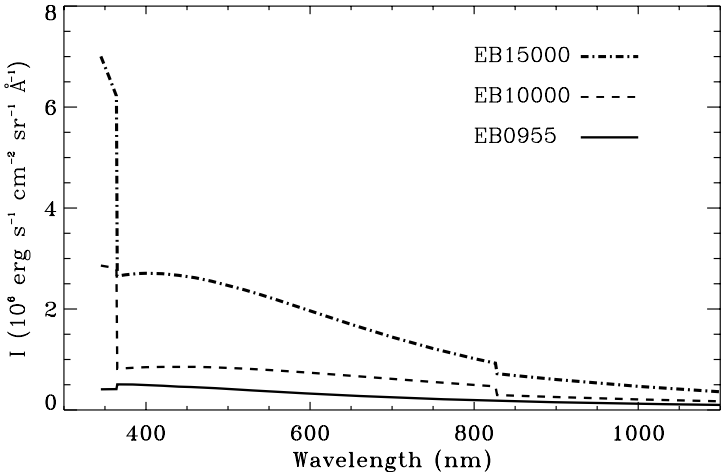

Fig. 3 Continuum emissions for the three EB models.

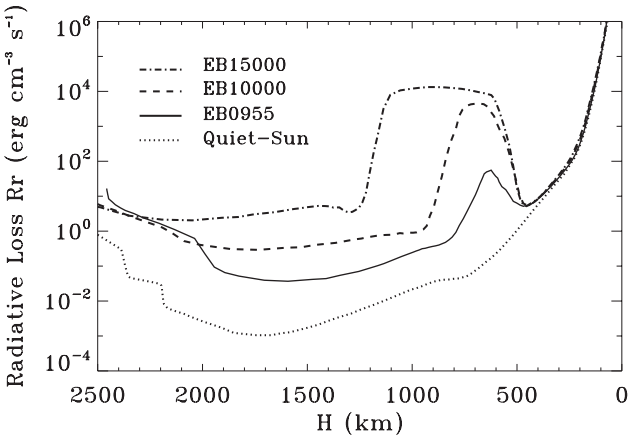

Fig. 4 Peak radiative losses for the three EB models.

losses changes during the EB lifetime D, we take 1/4 of the peak value as the mean rate. $A_{\rm EB}$ is the area of the EB. We use the empirical formula given by Jiang et al. (2010), which is a modification of the formula of Gan & Fang (1990) and is more suitable for small-scale activities. It is given as follows

$$R_{\rm r} = n_{\rm H} n_{\rm e} \Big[\alpha_1(h) + \alpha_2(h)\Big] f(T)\,. \qquad (2)$$

Here

$$\begin{aligned} \log\ \alpha_1(h) &= 1.745\times10^{-3}h - 4.739\,,\\ \alpha_2(h) &= 8.0\times10^{-2}{\rm e}^{-3.701\times10^{-2}h}\,,\\ f(T) &= 4.533\times10^{-23}(T/10^4)^{2.874}\,, \end{aligned}$$

where h is height in kilometers. Thus, using the non-LTE calculation results, we can obtain radiative losses for the three EB models.

Figure 4 gives the result. It is clear that the radiative losses of EB10000 and EB15000 are about two or three orders of magnitude higher than that of EB0955. This is due to their very high electron density in the lower atmosphere, which is caused by photoionization produced by high Balmer and Paschen emissions in the EB region, as shown in Figure 3.

Furthermore, if assuming that the main mechanism of energy loss is radiative, and taking the e-folding time of the maximum temperature decrease as the lifetime of the EBs, then, for a given energy E of an EB, we can estimate its lifetime by the formula

$$D = \frac{4\times E}{A_{\rm EB} R_{\rm EB}}\,. \qquad (3)$$

From the non-LTE calculation, we can obtain all necessary quantities for estimating the durations of the three EB models. For comparison, we assume that all the EBs have the typical size for EBs, $0.5'' \times 0.5''$. We take $h_1 = 337\,$km, and $h_2 = 2044\,$km for all three EBs. Considering the rapid decrease of hydrogen density with height, we neglect the contribution from the higher layers.

We take the total radiative energy $E = 1\times10^{26}\,$erg, which is a typical value for an EB (e.g. Fang et al. 2006; Li et al. 2015). Using Equation (3), we can estimate the lifetimes of the three EBs, which are listed in Table 1. It can be seen that the lifetimes of EB10000 and EB15000 would be two or three orders of magnitude shorter than that of EB0955, due to their very high radiative losses, which are not compatible with observations. Of course, for some very bright EBs the total radiative energy could be higher, say $1\times10^{27}\,$erg. In this case, the lifetimes of the high-temperature EBs are still very short. Moreover, for an EB having high temperature, the energy losses by heat conduction should be considered. It will decrease the EB lifetime further.

4 DISCUSSION AND CONCLUSIONS

Using non-LTE theory, we calculate the Hα and Ca II 8542 Å line profiles, as well as the continuum emissions, for three EB models with different temperatures around the TMR. Our results clearly reveal that the EB models with maximum temperature over 10 000 K will produce not only much stronger Hα and Ca II 8542 Å line profiles, but also very strong continuum emissions, particularly in the Balmer continuum. These line profiles and continuum emissions are not compatible with an EB model denoted as EB0955, which reproduces well the observations by BBSO/NST on 2013 June 6 at 09:55 UT.

Table 1 Characteristics of the Three EB Models

EB	Assumed size ($x \times y$) (arcsec)	$T_{\max}$ (K)	$R_{\rm EB}$ (erg cm^{-2} s^{-1})	Lifetime (s)
EB0955	0.5×0.5	7000	8.21×10^8	371
EB10000	0.5×0.5	10 000	7.26×10^{10}	4.19
EB15000	0.5×0.5	15 000	6.08×10^{11}	0.50

It should be emphasized that all these characteristics produced from EB10000 and EB15000 are never reported in EB spectral observations. Moreover, as mentioned above, we regard the e-folding time of the EBs as its lifetime, and the calculation is approximate since the radiative cooling rate changes non-linearly with temperature. Nevertheless, our results at least indicate that an EB with a temperature increase over 10 000 K around the TMR, if actually produced, cannot persist long enough with its high-temperature character. This certainly does not agree with EB observations. In other words, it is unlikely that the maximum temperature of EBs around the TMR could exceed 10 000 K. We notice that recently Reid et al. (2017) used the RADYN 1-dimensional radiative transfer code and concluded that the presence of superheated regions in the photosphere (>10 000 K) is not a plausible explanation for the production of EB signatures. This conclusion is consistent with our result.

It is thought that magnetic reconnection in the photosphere or lower chromosphere could be a mechanism for EBs (Ding et al. 1998; Georgoulis et al. 2002; Fang et al. 2006; Pariat et al. 2007; Isobe et al. 2007; Watanabe et al. 2011; Yang et al. 2013; Nelson et al. 2013). We have performed two-dimensional numerical MHD simulations on magnetic reconnection in the solar lower atmosphere (Chen et al. 2001; Jiang et al. 2010; Xu et al. 2011). Our results indicated that magnetic reconnection in the solar lower atmosphere can explain the temperature enhancement of about 600–3000 K and the lifetime of EBs. Recently, Ni et al. (2016) performed 2.5 dimensional MHD simulations which indicated that both high temperature ($\geq 8 \times 10^4$ K, if the plasma β is low) and low temperature ($\sim 10^4$ K, if β is high) events can happen around the TMR. However, they did not include the non-equilibrium ionization effect, which is certainly important for the high temperature case (Chen et al. 2001). Nevertheless, their result implies that high and low temperature events cannot happen at the same place. It is true that IBs need a high temperature of over 10 000 K to explain the enhanced EUV lines. However, according to our result, the maximum temperature of EBs around the TMR is unlikely to be higher than 10 000 K. This implies that IBs and EBs are unlikely to happen at exactly the same place. There are indeed some IBs that are closely connected to EBs in observations (e.g., Tian et al. 2016). They may reflect different temperature components that are produced by a common magnetic reconnection process. In fact, previous numerical simulations have revealed that both low and high temperature components can exist in the case of emerging flux reconnecting with a pre-existing magnetic field (Yokoyama & Shibata 1995; Jiang et al. 2012). Another possibility is that the jets produced by some EBs (see e.g. Nelson et al. 2015) could heat the upper atmosphere via waves or shocks. In this case, the high temperature region would be higher than the low temperature one. Then the apparent coincidence of both phenomena could only be due to the projection effect. For checking this point, a coordinated observation between IRIS and a large-aperture ground-based telescope targeting a region close to the limb may be useful. Anyway, for a clearer explanation of the relationship between EBs and IBs, we need more observations with higher spatial and temporal resolutions in the future.

Based on the analysis of three EB models, we draw the conclusion as follows:

According to our results from non-LTE calculation and semi-empirical modeling, it is unlikely that the maximum temperature of EBs around the TMR could exceed 10 000 K, otherwise the resulting Hα and Ca II 8542 Å line profiles, as well as the continuum emissions, would be too strong to be compatible with EB observations. Particularly, due to very high radiative losses in the high temperature models (EB10000 and EB15000), the lifetime of these events would be very short, which is inconsistent with any EB observations.

Acknowledgements We sincerely thank the anonymous referee for his/her valuable suggestions. This work is supported by the National Natural Science Foundation of China (NSFC, Grant Nos. 11533005, 11025314, 13001003, 11203014 and 11103075) as well as NKBRSF (Grant 2014CB744203).

References

Berlicki, A., & Heinzel, P. 2014, A&A, 567, A110

Cao, W., Gorceix, N., Coulter, R., et al. 2010, Astronomische Nachrichten, 331, 636

Chae, J., Park, H.-M., Ahn, K., et al. 2013, Sol. Phys., 288, 1

Chen, P.-F., Fang, C., & Ding, M.-D. D. 2001, ChJAA (Chin. J. Astron. Astrophys.), 1, 176

De Pontieu, B., Title, A. M., Lemen, J. R., et al. 2014, Sol. Phys., 289, 2733

Ding, M. D., Henoux, J.-C., & Fang, C. 1998, A&A, 332, 761

Ellerman, F. 1917, ApJ, 46, 298

Fang, C., Ding, M., Hénoux, J.-C., & Livingston, W. C. 2001, Science in China A: Mathematics, 44, 528

Fang, C., Tang, Y. H., Xu, Z., Ding, M. D., & Chen, P. F. 2006, ApJ, 643, 1325

Gan, W. Q., & Fang, C. 1990, ApJ, 358, 328

Georgoulis, M. K., Rust, D. M., Bernasconi, P. N., & Schmieder, B. 2002, ApJ, 575, 506

Goode, P. R., & Cao, W. 2012, in Proc. SPIE, 8444, Ground-based and Airborne Telescopes IV, 844403

Hong, J., Ding, M. D., Li, Y., Fang, C., & Cao, W. 2014, ApJ, 792, 13

Isobe, H., Tripathi, D., & Archontis, V. 2007, ApJ, 657, L53

Jiang, R. L., Fang, C., & Chen, P. F. 2010, ApJ, 710, 1387

Jiang, R.-L., Fang, C., & Chen, P.-F. 2012, ApJ, 751, 152

Kim, Y.-H., Yurchyshyn, V., Bong, S.-C., et al. 2015, ApJ, 810, 38

Li, Z., Fang, C., Guo, Y., et al. 2015, RAA (Research in Astronomy and Astrophysics), 15, 1513

Liu, Z., Xu, J., Gu, B.-Z., et al. 2014, RAA (Research in Astronomy and Astrophysics), 14, 705

Nelson, C. J., Doyle, J. G., Erdélyi, R., et al. 2013, Sol. Phys., 283, 307

Nelson, C. J., Scullion, E. M., Doyle, J. G., Freij, N., & Erdélyi, R. 2015, ApJ, 798, 19

Ni, L., Lin, J., Roussev, I. I., & Schmieder, B. 2016, ApJ, 832, 195

Pariat, E., Schmieder, B., Berlicki, A., et al. 2007, A&A, 473, 279

Peter, H., Tian, H., Curdt, W., et al. 2014, Science, 346, 1255726

Reid, A., Mathioudakis, M., Kowalski, A., Doyle, J. G., & Allred, J. C. 2017, arXiv:1701.04213

Rutten, R. J. 2016, A&A, 590, A124

Rutten, R. J., Vissers, G. J. M., Rouppe van der Voort, L. H. M., Sütterlin, P., & Vitas, N. 2013, in Journal of Physics Conference Series, 440, Journal of Physics Conference Series, 012007

Tian, H., Xu, Z., He, J., & Madsen, C. 2016, ApJ, 824, 96

Vernazza, J. E., Avrett, E. H., & Loeser, R. 1981, ApJS, 45, 635

Vissers, G., & Rouppe van der Voort, L. 2012, ApJ, 750, 22

Vissers, G. J. M., Rouppe van der Voort, L. H. M., Rutten, R. J., Carlsson, M., & De Pontieu, B. 2015, ApJ, 812, 11

Watanabe, H., Vissers, G., Kitai, R., Rouppe van der Voort, L., & Rutten, R. J. 2011, ApJ, 736, 71

Xu, X.-Y., Fang, C., Ding, M.-D., & Gao, D.-H. 2011, RAA (Research in Astronomy and Astrophysics), 11, 225

Yang, H., Chae, J., Lim, E.-K., et al. 2013, Sol. Phys., 288, 39

Yokoyama, T., & Shibata, K. 1995, Nature, 375, 42